Catalysis Today 74 (2002) 291–297

www.elsevier.com/locate/cattod

Selectivity and mechanism for skeletal isomerization of alkanes over typical solid acids and their Pt-promoted catalysts

Atsuyuki Miyaji, Tsuneo Echizen, Lianshun Li, Tetsuo Suzuki,
Yusuke Yoshinaga, Toshio Okuhara*

Graduate School of Environmental Earth Science, Hokkaido University, Sapporo 060-0810, Japan

Received 28 September 2001; received in revised form 12 November 2001; accepted 30 November 2001

Abstract

Selectivities for skeletal isomerizations of *n*-butane and *n*-pentane catalyzed by typical solid acids such as $Cs_{2.5}H_{0.5}PW_{12}O_{40}$ (Cs2.5), SO_4^{2-}/ZrO_2, WO_3/ZrO_2, and H-ZSM-5 and their Pt-promoted catalysts were compared. High selectivities for *n*-butane and low selectivity for *n*-pentane were observed over Cs2.5 and SO_4^{2-}/ZrO_2, while H-ZSM-5 was much less selective, and WO_3/ZrO_2 was highly selective for both reactions. The Pt-promoted solid acids were usually selective for these reactions in the presence of H_2 except for Pt-H-ZSM-5 for *n*-butane isomerization. Both the acid strength and pore structure would be factors influencing the selectivity. Mechanism of skeletal isomerization of *n*-butane was investigated by using 1,4-$^{13}C_2$-*n*-butane over Cs2.5 and Pt–Cs2.5. It was concluded that *n*-butane isomerization proceeded mainly via monomolecular pathway with intramolecular rearrangement on Pt–Cs2.5, while it occurred through bimolecular pathway with intermolecular rearrangement on Cs2.5. The higher selectivity on Pt–Cs2.5 would be brought about by the monomolecular mechanism. In the skeletal isomerization of cyclohexane, Pt–Cs2.5/SiO_2 was highly active and selective, while Pt–Cs2.5 was less selective. Control in the acid strength of Cs2.5 by the supporting would be responsible for the high selectivity.

Keywords: Skeletal isomerization; *n*-Alkane; Cyclohexane; Solid acid; Pt-promoted catalyst

1. Introduction

Skeletal isomerizations of *n*-alkanes are of industrially importance because the branched alkanes are generally useful as clean fuel. In addition, isobutane from *n*-butane is a raw material for alkylation with butenes to form clean gasoline (C8 branched alkanes), and the dehydrogenation product, isobutylene can be transformed into methyl *tert*-butyl ether (MTBE).

Although hydrocarbon-oils including aromatics like benzene are efficient gasoline having a high octane-number, it is keenly desirable to reduce the content of benzene in gasoline from a viewpoint of environmental protection. One possible way to diminish the benzene content in gasoline retaining its high octane-number is to transform benzene to methylcyclopentane by the hydroisomerization. Research octane-numbers of benzene and methylcyclopentane are 100 and 91, respectively, while those of cyclohexane and *n*-hexane are 83.0 and 25 [1]. Practically, the hydroisomerization of benzene has been operated in two-step processes consisting of hydrogenation of benzene and skeletal isomerization of product cyclohexane. Thus, the development of selective catalyst for the skeletal isomerization of cyclohexane is desired [2].

---

* Corresponding author. Tel./fax: +81-11-706-4513.
E-mail address: oku@ees.hokudai.ac.jp (T. Okuhara).

PII: S0920-5861(02)00031-7

In the present study, we chose the isomerizations of *n*-butane, *n*-pentane, and cyclohexane, and compared the catalytic features of various solid acids and the corresponding Pt-promoted catalysts for these reactions. Furthermore, to reveal the relation between the selectivity and the reaction mechanism, the mechanism for the *n*-butane isomerization was studied with 1,4-$^{13}C_2$-*n*-butane over Cs2.5 and Pt–Cs2.5 [3,4]. Although there are some reports about the mechanism using ^{13}C-labeled *n*-butane [5,6], quantitative discussion on the reaction pathways has not been performed because of the complex fragmentation in the composition analysis of ^{13}C-isobutane with a Mass spectroscopy. We used here an Field Ionization Mass analysis to make possible to determine the accurate ^{13}C-distribution of isobutane. As a result, the contribution of the monomolecular or bimolecular pathway has been quantitatively estimated.

2. Experimental

2.1. Catalysts

As solid acids, $Cs_{2.5}H_{0.5}PW_{12}O_{40}$, sulfated ZrO_2, H-ZSM-5, and WO_3/ZrO_2 were used. $Cs_{2.5}H_{0.5}PW_{12}O_{40}$ was prepared from aqueous solutions of $H_3PW_{12}O_{40}$ and Cs_2CO_3 by a titration method [7]. The surface area was 110 m^2 g^{-1} after the calcination at 523 K. This salt will be abbreviated as Cs2.5. Sulfated ZrO_2 was obtained from H_2SO_4 and Zr hydroxide by the calcination at 893 K for 5 h according to the literature [8]. The surface area was 90 m^2 g^{-1} after the calcination at 893 K in air. This will be denoted to SO_4^{2-}/ZrO_2. H-ZSM-5 was prepared by an ion-exchange of Na-ZSM-5 (Tosoh Corporation, HSZ-820NAA, Si/Al = 47). WO_3/ZrO_2 (W/Zr atomic ratio = 0.09) was prepared by an impregnation method using Zr hydroxide (Nippon Kigennso) and an aqueous solution of $(NH_4)_6W_7O_{24}$ [9]. The resulting solid was calcined at 1073 K (surface area: 47 m^2 g^{-1}).

Pt-promoted $Cs_{2.5}H_{0.5}PW_{12}O_{40}$ catalysts were prepared by the titration method [10,11]. An aqueous solution of $H_2PtCl_6\cdot 6H_2O$ (0.04 mol dm^{-3}) was added to an aqueous solution of $H_3PW_{12}O_{40}$ (0.08 mol dm^{-3}) at room temperature. Then an aqueous solution of Cs_2CO_3 (0.10 mol dm^{-3}) was added dropwise to the mixture at a rate of 0.1 cm^3 min^{-1} with vigorous stirring at room temperature. The obtained suspension was allowed to stand overnight at room temperature, and evaporated at 318 K to obtain solid. The loading amount of Pt was 2.0 wt.%. This catalyst will be denoted to Pt–Cs2.5. Silica-supported Pt–Cs2.5 was prepared from the aqueous solutions of Cs2.5 and $H_2PtCl_6\cdot 6H_2O$ using SiO_2 (Aerosil 300, 274 m^2 g^{-1}). The loading amounts of Pt and Cs2.5 were adjusted to 2 and 20 wt.%, respectively. This is denoted to Pt–Cs2.5/SiO_2. These heteropoly compounds were pretreated in a flow of O_2 for 2 h and then in a flow of H_2 for 1 h at 573 K. The Pt-promoted SO_4^{2-}/ZrO_2 was prepared by an incipient wetness impregnation with SO_4^{2-}/ZrO_2 and the aqueous solution of H_2PtCl_6. The obtained 2 wt.%Pt–SO_4^{2-}/ZrO_2 has 85 m^2 g^{-1} of the surface area after the calcination at 573 K for 2 h. 2 wt.%Pt–WO_3/ZrO_2 was prepared similarly with the aqueous solution of $H_2PtCl_6\cdot 6H_2O$ (0.04 mol dm^{-3}) by the impregnation method.

2.2. Catalytic reactions

For the isotopic experiment of *n*-butane isomerization, the reaction was carried out at 423–523 K in a closed circulation system (300 cm^3) with an on-line GC. The catalysts were pretreated in a vacuum at 573 K for 2 h (for Pt–Cs2.5 and Cs2.5) or at 673 K for 4 h (for Pt–SO_4^{2-}/ZrO_2 and SO_4^{2-}/ZrO_2). Then a mixture of 40 Torr (1 Torr = 133 Pa) of 1,4-$^{13}C_2$-*n*-butane (Isotec, ^{13}C: 99%) and 200 Torr of H_2 was introduced to the reaction system. The product isobutane and reactant *n*-butane were separated with a GC column (VZ-7) to be analyzed with a Field Ionization Mass Spectrometer (FI-MASS, JEOL JMS-SX102A) for ^{13}C-distribution. It should be emphasized that FI-MASS gave the parent peak patterns of isobutane and *n*-butane.

Skeletal isomerization of cyclohexane was carried out in a continuous flow system under an atmospheric pressure. The feed gas consisted of cyclohexane 12.4 vol.% and H_2 87.6 vol.%. Prior to the reaction, the catalysts were pretreated in a O_2 flow (50 cm^3 min^{-1}) for 2 h, in a He (50 cm^3 min^{-1}) for 10 min, and then in a H_2 flow (50 cm^3 min^{-1}) for 1 h at 573 K. The products were analyzed with an FID GC (Shimadzu GC-14B) equipped with a capillary column (WCOT Fused Silica Squalane).

Table 1
Selectivities for *n*-butane and *n*-pentane isomerizations over solid acids and their Pt-promoted catalysts

Catalyst	Selectivity to isobutane[a] (mol%)	Selectivity to isopentane[b] (mol%)
$Cs_{2.5}H_{0.5}PW_{12}O_{40}$	84.0–94.0 (473–573 K) [12]	20.0–58.5 (453–473 K) [13,14]
Pt–$Cs_{2.5}H_{0.5}PW_{12}O_{40}$	88.3–95.3 (473–573 K) [10,15–17]	96.4 (453 K) [13]
SO_4^{2-}/ZrO_2	60.7–97.5 (473–573 K) [12,18–20]	42.7–62.3 (473) [14,19]
Pt–SO_4^{2-}/ZrO_2	73.0–96.1 (473–573 K) [10,21,22]	91.6–99.6 (479–523 K) [13,23,24]
H-ZSM-5	14.1–28.3 (473–57 K) [12]	15.2–20.6 (523–453 K) [25]
Pt-H-ZSM-5	16.4–34.0 (573 K) [10,17]	91.9–93.9 (523–543) [25,26]
WO_3/ZrO_2	85.3–92.9 (573 K) [27]	91.3–97.3 (483–493 K) [28,29]
Pt–WO_3/ZrO_2	87.0–97.0 (623 K) [30]	95.5–98.9 (473 K) [31]

[a] Skeletal isomerization of *n*-butane.
[b] Skeletal isomerization of *n*-pentane.

3. Results and discussion

3.1. Selectivities for n-butane and n-pentane isomerizations

In Table 1, selectivities to isobutane in *n*-butane isomerization and isopentane in *n*-pentane isomerization over typical catalysts are summarized. Most of these data were collected from the literature [10,12–31]. In the cases of Pt-promoted catalysts, the reaction was performed in the presence of hydrogen. As can be seen in Table 1, the selectivity pattern was different depending on the catalyst system. The heteropoly compounds (Cs2.5 and Pt–Cs2.5) and sulfated ZrO_2 (SO_4^{2-}/ZrO_2 and Pt–SO_4^{2-}/ZrO_2) gave similar pattern; these catalysts are highly selective for *n*-butane isomerization and the Pt-promoted ones were also selective for *n*-pentane isomerization, while the solid acids (Cs2.5 and SO_4^{2-}/ZrO_2) were less selective for *n*-pentane isomerization. The lower selectivities for *n*-pentane isomerization over these solid acids were brought about by the cracking of oligomerized species to form C4, C5–C7 hydrocarbons. This cracking reaction is thought to proceed on the strong acid sites.

It is worthy to note that the *n*-pentane isomerization proceeded selectively over Pt-H-ZSM [25], while *n*-butane isomerization over H-ZSM-5 and Pt-H-ZSM-5 were not selective [10,12,17]. These low selectivities for *n*-butane isomerization over the zeolites are due to the influence of micropores [32]. On the other hand, we presume that the selective isomerization of *n*-pentane over Pt-H-ZSM-5 is attributed to the monomolecular pathway through a protonated dimethylcyclopropane intermediate.

Recent attractive catalysts are WO_3/ZrO_2 and Pt–WO_3/ZrO_2 [27–31]. As shown in Table 1, both the catalysts were selective for both reactions. As will be described below, WO_3/ZrO_2 possesses weak acid sites, which is responsible for the high selectivities. Another possibility has been proposed by Knozinger and coworkers [33], who claimed a radical intermediate for *n*-alkane isomerization on WO_3/ZrO_2.

3.2. Reaction mechanism for isomerization of n-butane

Recent mechanistic studies of *n*-butane isomerization using ^{13}C-*n*-butane [5,6] have pointed out that there are two possible pathways, i.e., bimolecular pathway which is accompanied with intermolecular rearrangement and monomolecular one with intramolecular rearrangement. Some studies about the mechanism were reported [5,6]. However, there is a controversy on the mechanism over SO_4^{2-}/ZrO_2 and quantitative discussion about the reaction pathways has not been performed. Adeeva et al. [5] inferred by using 1,4-$^{13}C_2$-*n*-butane that the skeletal isomerization occurred through the bimolecular mechanism, since the ^{13}C-distribution of product isobutane formed on SO_4^{2-}/ZrO_2 at 353 K was close to the binomial one. On the other hand, Garin et al. [6] reported using 1-$^{13}C_1$-*n*-butane that intramolecular rearrangement (monomolecular mechanism) was preferential over SO_4^{2-}/ZrO_2 at 523 K in the presence of H_2.

Possible reaction steps are illustrated in Scheme 1. If the reaction proceeds through the monomolecular pathway involving a protonated cyclopropane intermediate, the product isobutane would be $^{13}C_2$-isobutane,

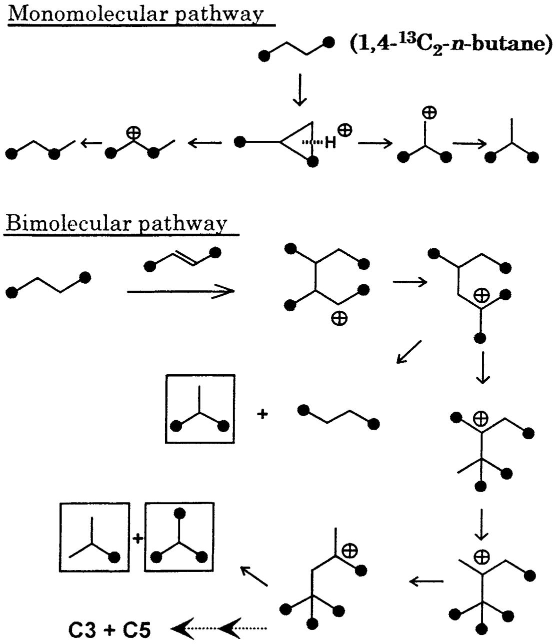

Scheme 1. Reaction pathways for skeletal isomerization of *n*-butane.

if the 1,4-$^{13}C_2$-*n*-butane was used as reactant. In addition, the high selectivity (100%) to isobutane is expected in this mechanism. On the other hand, the bimolecular mechanism would proceed accompanied with intermolecular rearrangement; a variety of isobutane having different numbers of ^{13}C would be formed from 1,4-$^{13}C_2$-*n*-butane (Scheme 1), because octyl cations readily undergo various rearrangements containing methyl shifts to give *tert*-carbenium ions.

Fig. 1 shows the isotopic distributions of isobutane formed over Pt–Cs2.5 and Cs2.5 at 423 K. Contrastive isotopic distributions were obtained between Pt–Cs2.5 and Cs2.5. Pt–Cs2.5 gave exclusively $^{13}C_2$-isobutane (Fig. 1A), but Cs2.5 brought about a spread distribution consisting of $^{13}C_0$-isobutane-$^{13}C_4$-isobutane. The isotopic distribution of isobutane formed over Cs2.5 (solid rectangles in Fig. 1B) was near close to the binomial distribution (open rectangles). It is noted that the fraction of $^{13}C_2$-isobutane in the observed pattern over Cs2.5 (Fig. 1B) was slightly higher than that of the calculated binomial distribution. It was confirmed that the reactant *n*-butane after the reaction was exclusively $^{13}C_2$-*n*-butane (not shown here) for all cases.

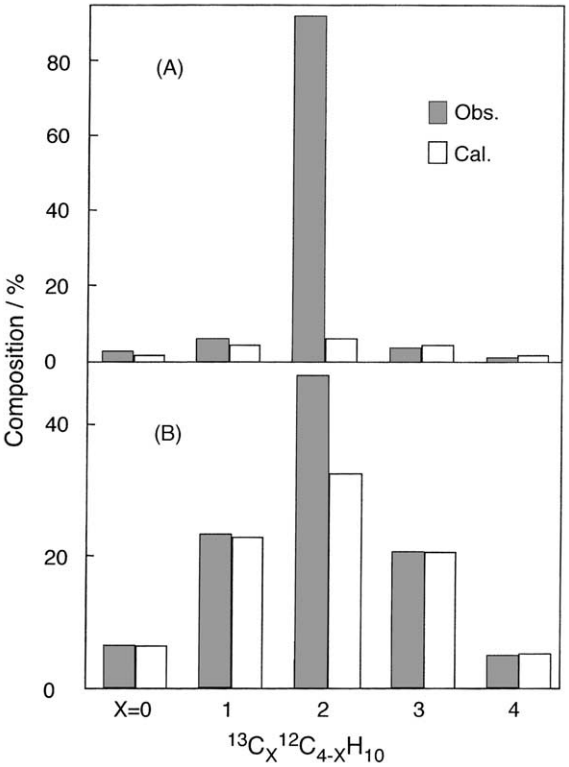

Fig. 1. ^{13}C-Distribution of isobutane in the isomerization of 1,4-$^{13}C_2$-*n*-butane over (A) 1.0 wt.%Pt–$Cs_{2.5}H_{0.5}PW_{12}O_{40}$ and (B) $Cs_{2.5}H_{0.5}PW_{12}O_{40}$ at 423 K.

We can estimate the contribution of each pathway from the difference between he observed fraction of $^{13}C_2$-isobutane and that of the binomial distribution, assuming that bimolecular path gives a binomial distribution and monomolecular path brings about only $^{13}C_2$-isobutane. In Table 2, the contributions of monomolecular pathway estimated from the above method are shown at the various reaction temperatures. It was found that the contribution of monomolecular pathway was 85.5% at 423 K and decreased to 63.3% at 523 K over Pt–Cs2.5. On the contrary, the contribution of the monomolecular pathway was 11.9% at 423 K and increased to 42.5% at 523 K over Cs2.5.

As shown in Tables 1 and 2, Pt–Cs2.5 was more selective than Cs2.5 in both reactions [10]. These differences in the selectivity are reasonably understood by the switching of the mechanism. The contribution of monomolecular pathway for *n*-butane isomerization was significant on Pt–Cs2.5 and the monomolecular

Table 2
The contribution of monomolecular pathway for *n*-butane isomerization

Catalyst	Temperature (K)	Conversion[a] (%)	Selectivity[b] (%)	Contribution[c] (%)
Pt–$Cs_{2.5}H_{0.5}PW_{12}O_{40}$	423	9.7	96.3	85.5
	453	27.8	96.6	75.8
	523	9.9	92.0	63.2
$Cs_{2.5}H_{0.5}PW_{12}O_{40}$	423	10.8	87.5	11.9
	423	22.0	86.7	12.8
	523	11.1	86.5	42.5

[a] At which the ^{13}C-distribution was measured.
[b] To isobutane.
[c] Contribution of monomolecular pathway.

pathway would exhibit 100% selectivity (Scheme 1). These are responsible for the higher selectivity of Pt–Cs2.5. The presence of Pt and H_2 might greatly suppress the formation of olefins and thus the bimolecular pathway would be intercepted. On the other hand, the bimolecular pathway was dominant over Cs2.5. Over Cs2.5 even in the presence of H_2, it is possible that butenes are formed from, e.g., deprotonation of butyl cation, since Cs2.5 does not possess the hydrogenation ability. These butenes would react readily with butyl cation to form octyl cations as intermediates in the bimolecular mechanism.

3.3. Skeletal isomerization of cylohexane

The skeletal isomerization of cyclohexane was examined using these Pt-promoted solid acids. Fig. 2 shows the time courses of skeletal isomerization of cyclohexane over various Pt-promoted solid acids. The conversion decreased slightly with time over all these catalysts, while among them, Pt–Cs2.5 was most deactivated. Stationary conversions were obtained at least after about 4 h over these catalysts. The selectivity to methylcyclopentane was significantly high over these catalysts except for Pt–Cs2.5 on which selectivity was about 97% under these conditions.

Fig. 3 gives *W*/*F* dependence of the conversion for the isomerization of cylohexane, where *W* is the catalyst weight and *F* the total flow rate for all the cases. While the conversion increased as the *W*/*F* increased, the slope of the curve became smaller at the high values of *W*/*F*. The reaction rates were calculated from the slopes of the linear portions of the curves at the conversions less than 20%.

The selectivity to methylcyclopentane is plotted against the conversion in Fig. 4. It was found that the selectivities over Pt–WO_3/ZrO_2 and Pt–Cs2.5/SiO_2 were almost 100% up to about 50% conversions. The equilibrium conversion is about 70%, when only the skeletal isomerization took place. Contrary to the above catalysts, Pt–Cs2.5 and Pt–SO_4^{2-}/ZrO_2 were less selective. The by-products observed over Pt–Cs2.5 contained C7 and C8 hydrocarbons, together with C4 and C5. Thus the oligomerization of the corresponding olefins and cracking of the oligomer brought about mainly these by-products. The selectivities and the reaction rates are summarized in Table 3.

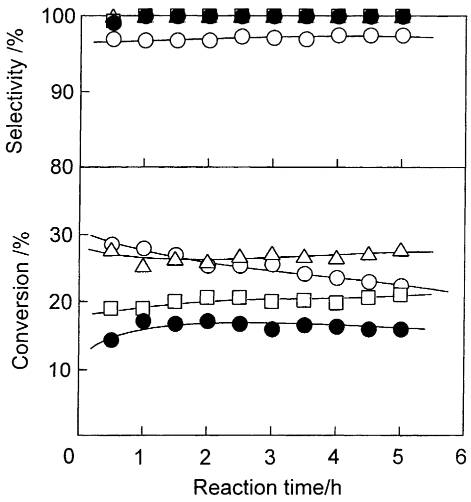

Fig. 2. Time courses for isomerization of cyclohexane over Pt-promoted solid acids at 473 K. (○): Pt–$Cs_{2.5}H_{0.5}PW_{12}O_{40}$, (△): Pt–Cs2.5/$SiO_2$, (□): Pt–$SO_4^{2-}/ZrO_2$, (●): Pt–$WO_3/ZrO_2$. $W/F = 10$ g-cat h mol^{-1}.

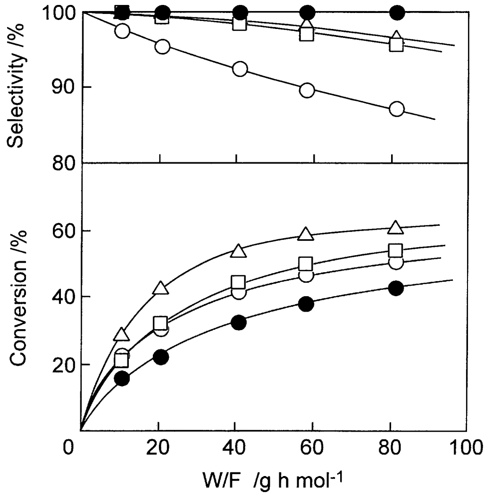

Fig. 3. *W*/*F* dependence of the conversion of cyclohexane isomerization. (○): Pt–$Cs_{2.5}H_{0.5}PW_{12}O_{40}$, (△): Pt–Cs2.5/$SiO_2$, (□): Pt–$SO_4{}^{2-}$/$ZrO_2$, (●): Pt–$WO_3$/$ZrO_2$.

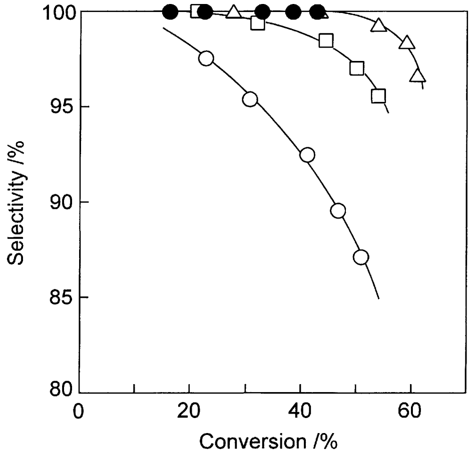

Fig. 4. Selectivity to methylcyclopentane as a function of conversion for isomerization of cyclohexane. (○): Pt–$Cs_{2.5}H_{0.5}PW_{12}O_{40}$, (△): Pt–Cs2.5/$SiO_2$, (□): Pt–$SO_4{}^{2-}$/$ZrO_2$, (●): Pt–$WO_3$/$ZrO_2$.

Table 3 demonstrates that Pt–Cs2.5/SiO_2 was most active with the high selectivity to methylcyclopentane. It should be further emphasized that the activity of Cs2.5 increased by the supporting Cs2.5 on SiO_2 about seven times.

As reported previously [2], the isomerization of cyclohexane is the slow step for the hydroisomerization of benzene over Pt–Cs2.5. For this step, the strong acids and the large amount of acid site are favorable. However, when the acid strength is too high, the cracking would be accelerated to form the by-products. Thus the acid strength may be critical for the selectivity. The very high selectivity was detected on Pt–WO_3/ZrO_2, while the activity was moderate. As Fig. 5 shows, ammonia was desorbed at lower temperature from the surface of WO_3/ZrO_2 than that from Cs2.5. This result indicates that the acid strength of WO_3/ZrO_2 was lower than that of Cs2.5, which is a reason for the high selectivity to methylcyclopentane. The peak of NH_3 desorption was slightly shifted to lower temperature when Cs2.5 was supported on SiO_2, indicating that the acid strength became lower by the supporting. This is consistent with the decreasing in the acid strength of $H_3PW_{12}O_{40}$ by supporting [34]. The lowering the acid strength of Cs2.5 on SiO_2 would bring about the high selectivity.

Table 3
Reaction rates and selectivity for isomerization of cyclohexane

Catalyst[a]	Rate (mmol g_{cat}^{-1} h^{-1})	Selectivity[b] (%)					
		C1–C3	C4	C5	C6	MCP[c]	C7–C8
Pt–$Cs_{2.5}H_{0.5}PW_{12}O_{40}$	30	0	5.5	4.0	2.4	87.6	0.5
Pt–Cs2.5/SiO_2	44	0	0.9	0.3	0	96.7	2.1
Pt–$SO_4{}^{2-}$/ZrO_2	28	0	0.6	0.3	0.6	95.5	3.1
Pt–WO_3/ZrO_2	19	0	0	0	0	100	0

[a] The loading amount of Pt was 2 wt.%.

[b] 100 × *n*[Cn]/[total carbon atom], where [Cn] and [total carbon atom] mean the concentrations of a hydrocarbon having *n* carbon atom and total carbon atom, respectively.

[c] Methylcyclopentane.

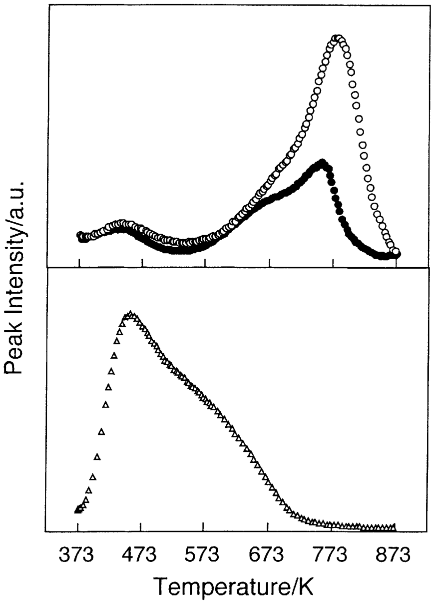

Fig. 5. NH$_3$ TPD from solid acids. (○): Cs$_{2.5}$H$_{0.5}$PW$_{12}$O$_{40}$, (●): Cs2.5/SiO$_2$, (△): WO$_3$/ZrO$_2$. Ammonia (100 Torr) was introduced to the catalyst at 373 K for 10 min, and was evacuated for 30 min. The temperature of the catalyst was raised with 10 K min^{-1} in vacuum.

Acknowledgements

This work has been carried out as a research project of the Japan Petroleum Institute commissioned by the Petroleum Energy Center with the subsidy of the Ministry of Economy, Trade and Industry. This study was also partly supported by Grant-in-Aid for Scientific Research from the Ministry of Education, Science, Sports, and Culture, Japan.

References

[1] C.N. Satterfield, Heterogeneous Catalysis in Practice, McGraw-Hill, New York, 1980.
[2] R. Watanabe, T. Suzuki, T. Okuhara, Catal. Today 66 (2001) 123.
[3] T. Suzuki, T. Okuhara, Chem. Lett. (2000) 470.
[4] T. Suzuki, T. Okuhara, Catal. Lett. 72 (2001) 111.
[5] V. Adeeva, G.D. Lei, W.M.H. Sachtler, Catal. Lett. 33 (1995) 135; V. Adeeva, G.D. Lei, W.M.H. Sachtler, Appl. Catal. 118 (1994) L11.
[6] F. Garin, L. Seyfried, P. Gitard, G. Maire, A. Abdulsamad, J. Sommer, J. Catal. 151 (1995) 26.
[7] T. Okuhara, H. Watanabe, T. Nishimura, K. Inumaru, M. Misono, Chem. Mater. 12 (2000) 253.
[8] M. Hino, K. Arata, Catal. Lett. 30 (1995) 25.
[9] L. Li, Y. Yoshinaga, T. Okuhara, Phys. Chem. Chem. Phys. 1 (1999) 4913.
[10] K. Na, T. Okuhara, M. Misono, J. Catal. 170 (1997) 96.
[11] Y. Yoshinaga, T. Okuhara, J. Chem. Soc., Faraday Trans. 94 (1998) 2235.
[12] K. Na, T. Okuhara, M. Misono, J. Chem. Soc., Faraday Trans. 91 (1993) 367.
[13] Y. Liu, K. Na, M. Misono, J. Mol. Catal. A 141 (1999) 145.
[14] T. Suzuki, T. Okuhara, Unpublished data.
[15] T. Okuhara, T. Yamada, K. Seki, K. Johkan, T. Nakato, Microporous Mesoporous Mater. 21 (1998) 637.
[16] K. Na, T. Iizaki, T. Okuhara, M. Misono, J. Mol. Catal. A 115 (1997) 449.
[17] K. Na, T. Okuhara, M. Misono, J. Chem. Soc., Chem. Commun. (1993) 1422.
[18] F.R. Chen, G. Coudurier, J.F. Joly, J.C. Vedrine, J. Catal. 143 (1993) 616.
[19] B.B. Bardin, R.J. Davis, Top. Catal. 6 (1998) 77.
[20] A. Corma, V. Fornes, M.I. Juan-Rajadell, J.M. Lopez Nieto, Appl. Catal. A 116 (1994) 151.
[21] K.J. Chao, H.C. Wu, L.J. Leu, J. Catal. A 157 (1996) 289.
[22] J.C. Yori, M.A. D'Amato, G. Costa, J.M. Parera, J. Catal. 153 (1995) 218.
[23] H. Liu, G.D. Lei, W.M.H. Sachtler, Appl. Catal. A 146 (1996) 165.
[24] K. Ebitani, J. Konishi, H. Hattori, J. Catal. 130 (1991) 257.
[25] K. Fujimoto, K. Maeda, K. Aimoto, Appl. Catal. A 91 (1992) 81.
[26] A. Zhang, I. Nakamura, K. Aimoto, K. Fujimoto, Ind. Eng. Chem. Res. 34 (1995) 1074.
[27] J.C. Yori, C.L. Pieck, J.M. Parera, Appl. Catal. A 181 (1999) 5.
[28] J.G. Santiesteban, J.C. Vartuli, S. Han, R.D. Bastian, C.D. Chang, J. Catal. 168 (1997) 431.
[29] J.C. Vartuli, J.G. Santiesteban, P. Traverso, N. Cardona-Martinez, C.D. Chang, S.A. Stevenson, J. Catal. 187 (1999) 131.
[30] J.C. Yori, J.M. Parera, Catal. Lett. 65 (2000) 205.
[31] J.G. Santiesteban, D.C. Calabro, W.S. Borghard, C.D. Chang, J.C. Vartuli, Y.P. Tsao, M.A. Natal-Santiago, R.D. Bastian, J. Catal. 183 (1999) 314.
[32] T. Okuhara, Y. Yoshinaga, R. Watanabe, Am. Chem. Soc. Book 738 (1999) 369.
[33] S. Kuba, P.C. Heydorn, R.K. Grasselli, B.C. Gates, M. Che, H. Knozinger, Phys. Chem. Chem. Phys. 3 (2001) 146.
[34] G.I. Kapustin, T.R. Brueva, A.L. Klachko, M.N. Timofeeva, S.M. Klikov, I.V. Kozhevnikov, Kinet. Katal. 31 (1990) 896.